POAC'11
Montréal, Canada

Proceedings of the 21st International Conference on
Port and Ocean Engineering under Arctic Conditions
July 10-14, 2011
Montréal, Canada

POAC11-004

Integrated numerical analysis of iceberg collisions with ship sides

Zhenhui Liu [1*], Jørgen Amdahl[2],Sveinung Løset[3]

[1]Reinertsen AS, Trondheim, Norway

[2]Department of Marine Technology, Norwegian University of Science and Technology, Trondheim (NTNU), Norway

[3]Department of Civil and Transportation Engineering, Norwegian University of Science and Technology, Trondheim (NTNU), Norway

ABSTRACT

This paper deals with the integrated numerical analysis of iceberg collisions with ship sides. A nonlinear explicit commercial code LS-DYNA 971 was used in the analysis. The deformations and fracture of both the ship structure and iceberg are considered. The *RTCL* failure criterion is applied to simulate steel fracture, whereas the iceberg fracture model is simulated by a plastic strain and pressure-based empirical failure criterion. Material models for steel and iceberg are implemented in the commercial code through a user-defined subroutine. For simplicity, the ship-iceberg collision is split into external and internal mechanics. Thus, only part of the ship structure and iceberg is modelled in the numerical simulations. The ship structure is based on the drawings of an ice-strengthened FPSO, and only the side structure is modelled. The structure model has been enlarged to minimise boundary influences. Different shapes for the leading edges of the iceberg are proposed, namely so-called "sharp", "blunt" and "intermediate" icebergs. The iceberg shapes are simply represented by revolving a parabolic or circular profile line about its symmetry axis. Four profiles are proposed. Three different collision locations were simulated as well. Rigid analyses have also been performed. Finally, 24 numerical simulations have been carried out. The results for the maximum deflection of the outer and inner shells and the total internal energy are presented. Discussions and conclusions based on the results are provided as well.

Introduction

Arctic waters are attracting researchers and engineers due to the large reserves of oil and gas and the potential for new sailing routes through this area. It is expected that ship traffic will increase in this area in the near future. Thus, the probability of ship/iceberg collision increases, and it is necessary to investigate ship and iceberg collision problems in Arctic and sub-Arctic waters. This paper presents a study on the numerical simulation of iceberg collisions with ship sides.

---

[*] This work was conducted when the first author worked at NTNU as Ph.D. candidate.

To simplify the ship-iceberg collision, the division of external and internal mechanics is recommended; see Pedersen and Zhang [1]. The external mechanics describe translational and rotational momentum balance and energy dissipation. Recently, Liu and Amdahl [2] developed a new formulation for the external mechanics of ship-ship collisions. It is also applicable to ship-iceberg collisions. With the given information about the mass, velocities, added mass factors and ship/iceberg shape properties, the total dissipated energy for a ship-iceberg collision scenario can be efficiently obtained. On the other hand, the internal mechanics of ship-iceberg collision focus on the local deformations of both the ship and iceberg. *Nonlinear finite element analyses* (*NLFEA*) are always used to access the internal mechanics. Due to the large deformations, *NLFEA* should be able to handle the fracture of both steel and ice. The external and internal mechanics are linked to one another by the dissipated energy. By dividing the external and internal mechanics, models of the entire ship and iceberg are not required in the *finite element model (FEM).* The examples of this can be found in paper by Liu *et.al.* [3,4]. Figure 1 shows an illustration of this simplification. The computational time is significantly reduced by following this principle. More effort can then be focused on detailed studies of the internal mechanics.

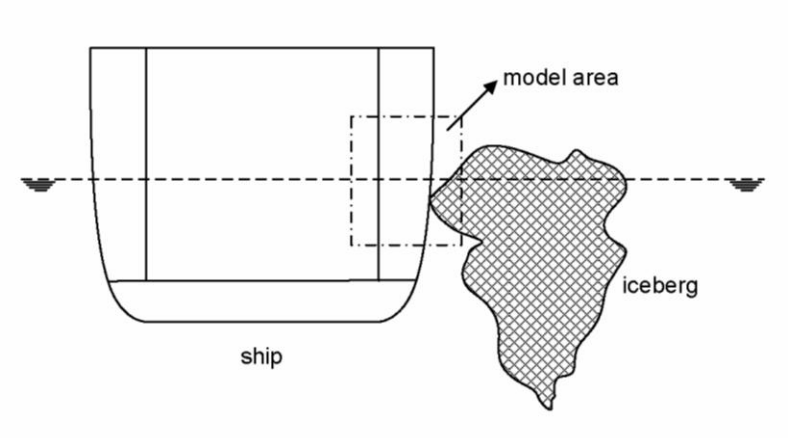

Figure 1. Illustration of side-ship and iceberg collision (cross-sectional view).

Ship and iceberg models

Ship structure

The ship structure model used in this study is based on the side scantlings of a FPSO tanker, which has been designed for ice loads. The main dimensions are listed in Table 1.

Table 1. Main dimensions.

Location	Stiffener/web Frame	Spacing [mm]	Frame/stringer spacing [mm]	Plate thickness [mm]	Material stiffener [MPa]	Material plating [MPa]
Side	250 x 12 BP	600	4430/2215	23	285	285
Inner	450 x 125 BP	825	4430	17	285	285

To minimise the influence of the boundary conditions set for the structural model, the model described above was arrayed into a 3 x 3 matrix as shown in Figure 2. The

boundary conditions are defined according to Table 2, where 1 denotes fixed and 0 indicates free (see also Figure 2).

Table 2. Boundary conditions.

Location	X	Y	Z	RX	RY	RZ
Boundary A	1	0	1	0	0	0
Boundary B	1	1	0	0	0	0

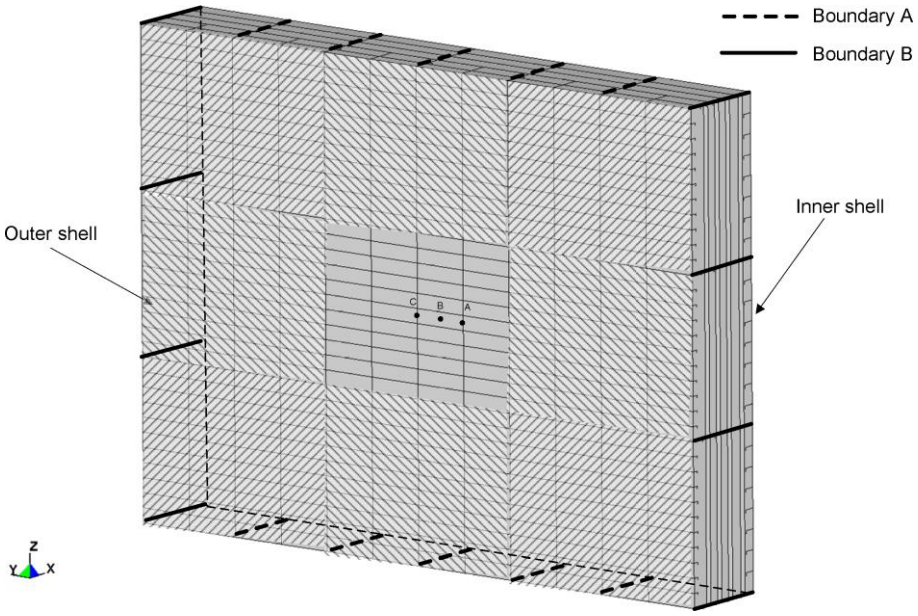

Figure 2. The side structure model with illustrations of the boundary conditions and collision locations.

The structure model was meshed by using a Belytschko-Tsay quadrangular mesh with a general mesh size of 120 mm × 120 mm. The material model for steel in this study should be able to predict the fracture and crack propagation of steel. Thus, the material model developed by Alsos et al. (2009) [5] is employed here. The power law expression was chosen to describe the stress-strain relationship. In this study, $\sigma_Y = 285$, $K = 740$, $n = 0.24$. The so-called *RTCL* (Rice–Tracey and Crockcroft–Latham) failure criterion was adopted in the material code for steel in which the triaxiality is considered; more information is provided in a paper by Alsos et al. [5].

Iceberg profile

As previously discussed, only the local area of contact with the iceberg is required in the numerical simulations. However, it is still a great challenge to model the correct shape of contact area. Similar problems have been discussed by Alsos and Amdahl [6] with respect to ship grounding They defined three categories of seabed topology on the basis of the extent of damage, namely rock, reef and shoal. Similarly, we may also consider categorising the iceberg profile based on the extent of structural damage.

Generally, two categories of iceberg profiles, “sharp” and “blunt”, are proposed. Both “sharp” and “blunt” can be simply represented by revolving a parabolic or a circle profile line about its symmetry axis. As shown in Figure 3, the iceberg profiles based on different parabolic or circular lines are created. The 3D iceberg shapes can be

easily obtained by revolving the profile lines 360° about the X-axis. In this paper, the iceberg shapes were modelled based on the parabolic line $X = -\frac{1}{500}Y^2$ and half-circle lines, $Y^2 + (X + r)^2 = r^2$, where r equals 1000 mm, 2000 mm and 3000 mm. All of the icebergs modelled have the same height of 2000 mm along the X-axis. Thus, a round platform was additionally attached to the half sphere when $r = 1000\,\text{mm}$ with an inclination angle of 25^0. The final iceberg shapes are presented in Figure 4.

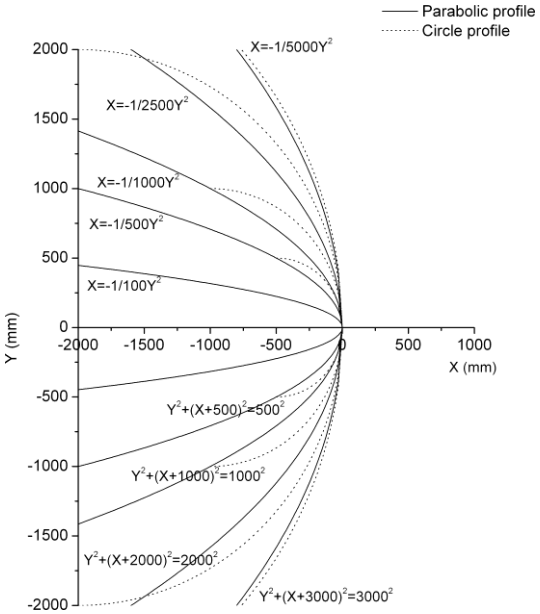

Figure 3. Iceberg profiles presented by parabolic and circle lines.

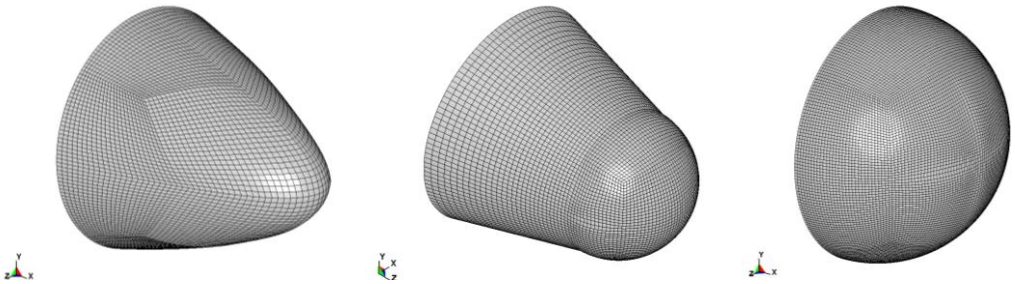
Figure 4. FEM models for local iceberg part (parabola, round platform plus half-sphere and sphere).

The 3D iceberg models were all meshed by hexahedral elements with mesh size of 50 mm x 50 mm x 50 mm. The material model used here is that presented by Liu et al. [6]. The inputs applied to the ice material model are: a_0 =22.93, a_1 =2.06, a_2 =-0.023, $p_{cut} = -2\,MPa$, $\varepsilon_0 = 0.01$, where a_0, a_1, a_2, p_{cut} and ε_0 are constants defining the material model. The iceberg material model was developed to facilitate the iceberg impact simulations by authors. It is based on the so called '*Tsai-Wu'* yield surface and a user-defined failure criterion. The failure is dependent on pressure and plastic strain of the elements; more information is available in a paper by Liu *et. al.* [7]. In addition to the integrated analysis, rigid icebergs are also included. For the rigid analysis, it is not necessary to use a solid-element mesh; the Belytschko-Tsay quadrangular mesh is used for the outer shell of the above icebergs' instead.

Collision location

The locations of initial contact during the ship-iceberg collision are assumed to be in the middle of the structure model; thus, the influence of the boundary conditions is minimised. Three typical locations are proposed, as seen in Figure 2. If we considered a grid (2215 mm × 600 mm) between the stringer/web frame and two longitudinal stiffeners, the three points A, B and C are distributed evenly along this grid.

Results

All of the simulations were carried out by the computer code LS-DYNA 971. There were three contacts defined in the simulations, as listed in Table 3. In total, 24 numerical cases are summarised in Table 4. The iceberg was simulated to move against the ship structure at a constant velocity of 4000 mm/s, and the maximum penetration was set to 2000 mm.

Table 3. Contact and friction definition.

	Contact location	Contact algorithm	Friction
1	Ship structure and iceberg	*CONTACT_ERODING_SURFACE_TO_SURFACE	0.15
2	Ship structure	*CONTACT_AUTOMATIC_SINGLE_SURFACE	0.30
3	Iceberg	*CONTACT_ERODING_SINGLE_SURFACE	0.15

Table 4. Summary of all numerical cases.

No.	Name	Integrated or Rigid analysis	Iceberg profiles	Location
1	I-P-500-A	Integrated	Parabolic line $X = -\frac{1}{500}Y^2$	A
2	R-P-500-A	Rigid	Parabolic line $X = -\frac{1}{500}Y^2$	A
3	I-C-1000-A	Integrated	Circle line $Y^2 + (X - 1000)^2 = 1000^2$	A
4	R-C-1000-A	Rigid	Circle line $Y^2 + (X - 1000)^2 = 1000^2$	A
5	I-C-2000-A	Integrated	Circle line $Y^2 + (X - 2000)^2 = 2000^2$	A
6	R-C-2000-A	Rigid	Circle line $Y^2 + (X - 2000)^2 = 2000^2$	A
7	I-C-3000-A	Integrated	Circle line $Y^2 + (X - 3000)^2 = 3000^2$	A
8	R-C-3000-A	Rigid	Circle line $Y^2 + (X - 3000)^2 = 3000^2$	A
9	I-P-500-B	Integrated	Parabolic line $X = -\frac{1}{500}Y^2$	B
…	…	…	…	…
24	R-C-3000-C	Rigid	Circle line $Y^2 + (X - 3000)^2 = 3000^2$	C

Figure 5 shows the iceberg damage patterns in the integrated analysis. The “sharp” (the first group, e.g., Figure 5(a) I-P-500-A) iceberg is mostly deformed, while the “blunt” (the last group, e.g. Figure 5(d) I-C-3000-A) iceberg is only slightly deformed. A moderate extent of deformation is observed for shapes intermediate between “sharp” and “blunt” (second and third group, e.g., I-C-1000-A and I-C-2000-A). The rigid analysis simulation was also carried out for the sake of comparison. Significant differences were observed, which point to the necessity of conducting integrated analyses of ship and iceberg collision scenarios. The following sections will present detailed results.

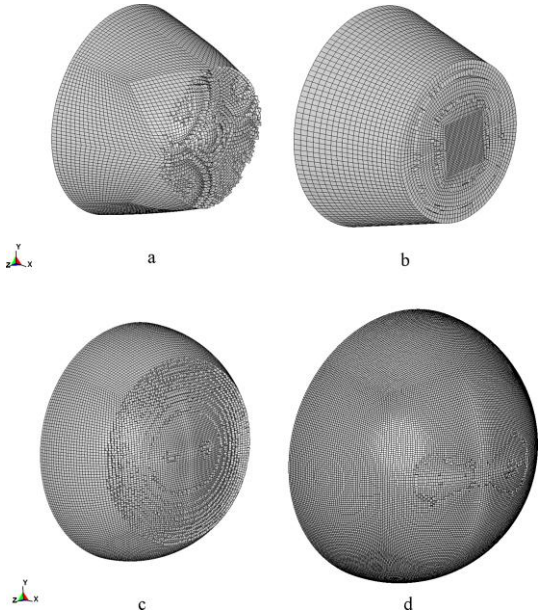

Figure 5. Iceberg damage patterns: a, Case 1, I-P-500-A, b, Case 3, I-C-1000-A, c, Case 6, I-C-2000-A, d, Case 9, I-C-3000-A.

Maximum deformation of outer and inner shell

The maximum deflections of the outer shell for all simulations are summarised in Figure 6. For the rigid analysis cases, the maximum deflection should be equal to the iceberg displacement; see the black line in Figure 6. In most cases, the integrated analyses are quite different from those corresponding to the rigid analyses. The difference becomes more obvious when the iceberg is "sharper", as the iceberg is quite easily crushed. The deflection of the structure in the integrated analyses is much smaller than that under the rigid analyses, e.g., cases I-P-500-A,B,C. It is interesting to note that the location of collision shows significant influence on the extent of damage of the side structure, e.g., cases I-C-1000-B and I-C-2000-B. The collision at location B in both cases produces much more damage to the side structure, while other two locations are less damaged. Location B is less supported than A and C, as shown in Figure 2. The detailed failure pattern in such cases is illustrated in Figure 7 for case I-C-1000-B. Initially, the iceberg is sufficiently stiff to crush the side structure; however, the relative stiffness changes when the iceberg is in contact with the web frame and the stringer. The support from the web frames and stringers increases the side structure's ability to crush the iceberg.

The differences between the integrated and rigid analyses for cases I-C-2000-A,B,C and I-C-3000-A,B,C are quite small. The side structure is not able to crush this size or shape of iceberg. Fracture is only observed in the first two groups of rigid analyses, e.g., R-P-500-A,B,C and R-C-1000-A,B,C. In cases R-P-500-A,B,C, the "sharp" iceberg penetrates the outer shell of the side structure during the early stage of collision (see the star symbol in Figure 6). For cases R-C-1000-A,B,C, the fracture is initiated when the iceberg penetration distance is approximately 1000 mm.

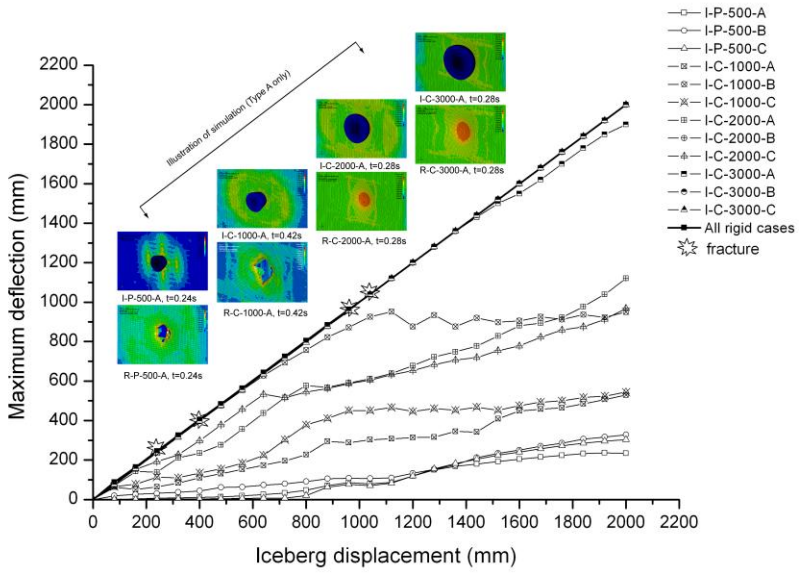

Figure 6. Maximum deflections of outer shell with iceberg displacement.

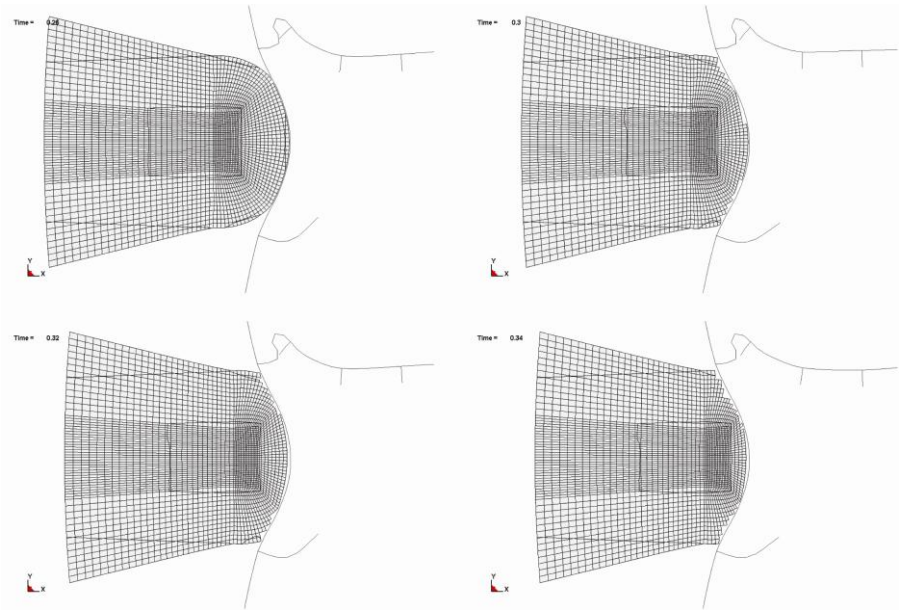

Figure 7. Horizontal cross-sections for case I-C-1000-B at different time frames.

The deflection of the inner shell is of great interest as it is an important criterion in judging a ship's survivability, especially for membrane-type LNG ships. The maximum deflection of the inner shell in the present research was only as high as 265 mm. Figure 8 summarises the maximum inner shell deflections for all cases. Only small differences are found between the integrated and rigid analyses in the first two groups (I-P-500-A,B,C, R-P-500-A,B,C and I-C-1000-A,B,C, R-C-1000-A,B,C), where fractures are observed. For the integrated analyses, the side structure crushes the iceberg ice and the inner shell experiences quite a small deflection, while for the rigid analyses, the side structure is penetrated by the iceberg, and large parts of the energy dissipation are focused in local areas where the rigid iceberg is in contact with it. Thus, the inner shell is still less influenced in such cases. However, it can be expected that the inner shell may be penetrated by the rigid iceberg if the iceberg displacement is sufficiently long. Another observation is that the deflection of the

inner shell in these two groups shows vibrations; this is due to the crushed ice that has been eroded in the simulation in the integrated cases and the fracture of the outer shell in the rigid cases. When the iceberg curvature becomes smaller, for example, in cases I-C-2000-A,B,C and R-C-2000-A,B,C, the difference is significant, as shown in Figure 8. For cases I-C-2000-A and I-C-2000-C, the collision is located where web frames and stringers are laid; the iceberg is crushed due to the strong support, and thus, the inner shell deflection is quite less than the deflections of the corresponding rigid analyses. The reason for this is the same as that discussed in the previous subsection. The differences between the integrated and rigid analyses for cases I-C-3000-A,B,C are quite small, indicating that the icebergs are sufficiently stiff to crush the side structure.

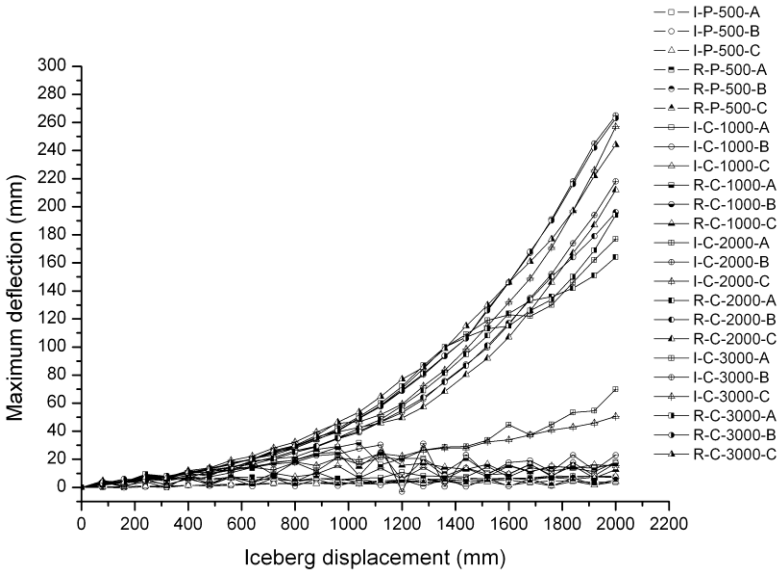

Figure 8. Maximum deflection of inner shell with penetration distance.

Energy dissipation ratio discussion

To illustrate the difference between the integrated and rigid analyses, the total internal energy dissipation during the collision was assessed. The total internal energy includes the eroded internal energy, as we have element erosion in most cases.

The total internal energy for the integrated analyses is normalised to that of the corresponding rigid analyses, as shown in Figure 9. The internal energy ratio in the first group (I-P-500-A,B,C) is far from being 1, which can only be described by the integrated analyses. The rigid analyses in such cases (“sharp”) may overestimate the internal energy and produce a design that is too conservative. The ratio in this group increases with the penetration distance, which indicates the increasing stiffness of the iceberg. The second and third group (I-C-1000-A,B,C and I-C-2000-A,B,C) show the same trend. The internal energy ratios for types A and C are smaller than 1 and almost equal to 1 for type B in both groups in which the points of collision are located in less-supported areas.

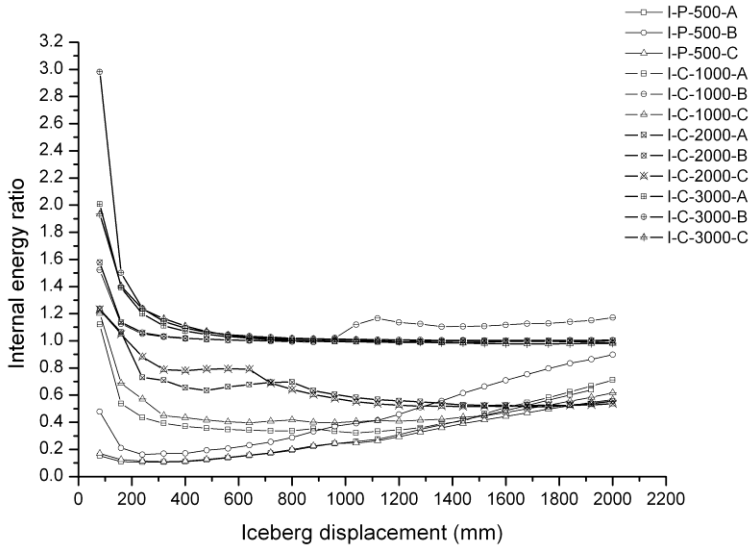

Figure 9. Internal energy ratio between the integrated and rigid analyses.

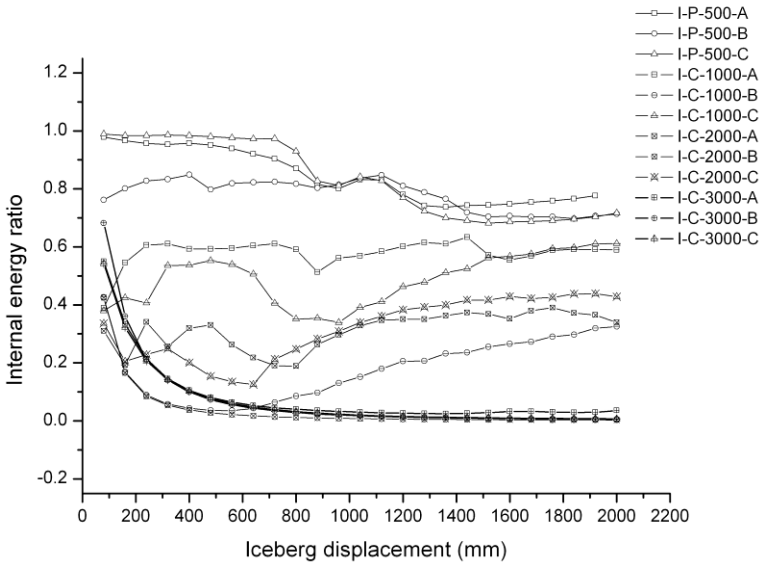

Figure 10. Internal energy ratio between icebergs and the total energy for integrated analyses.

Another interesting feature is shown in Figure 10. The internal energy ratio between the iceberg and the total energy is summarised for all of the integrated analyses. A ratio equal to 1 indicates that the internal energy goes to the iceberg, while the side structure is intact and has no contribution; on the contrary, if the ratio equals 0, then the side structure endures the deformation, while the iceberg remains stiff. It is shown that the internal energy ratio is close to 1 in the first group (I-P-500-A, B, C), where the iceberg is crushed, and the structure is kept intact. The influence of the collision location is also observed. The second group (I-C-1000-A,B,C) shows that the iceberg and the structure contribute almost equally to the total internal energy, except for case I-C-1000-B where the side structure is less supported. The ratio in the third group (I-C-2000-A, B, C) is smaller than 0.5, which means that the side structure contributes more than the iceberg to the internal energy. The iceberg is becoming stiff and more of

the structure is crushed. The iceberg in case I-C-2000-B is almost as stiff as it is rigid as the ratio is close to 0. The last group (I-C-3000-A, B, C) shows that the iceberg in this scenario is almost the same as that in the rigid case. All of the internal energy is contributed by the side structure.

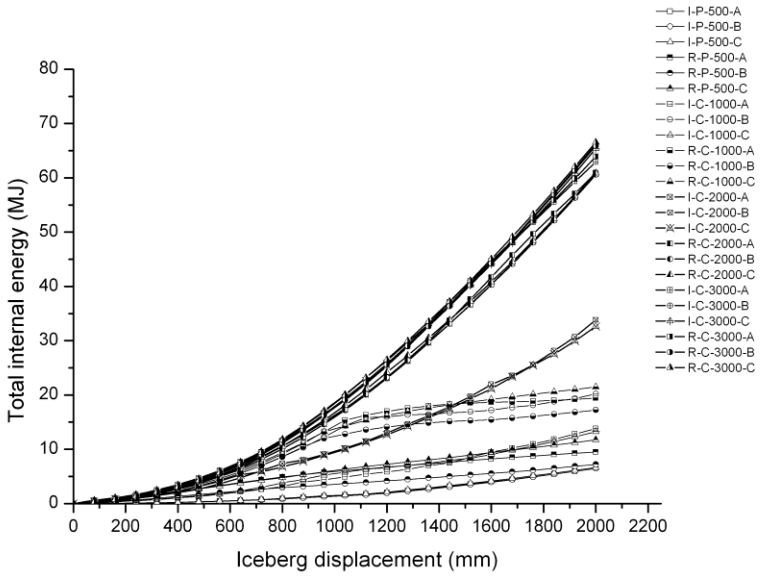

Figure 11. Total internal energy with the iceberg displacement for all cases.

Discussion and conclusions

The results presented previously show the details of the integrated and rigid analyses, which are mainly focused on the internal mechanics, local deformations and energy dissipation. To place the internal mechanics into a practical context, the introduction of the external mechanics is necessary. Figure 11 shows the values of the total internal energy for all cases analysed. Based on these results, we consider case I-P-500-B as an example. The total internal energy is 6.5 MJ at a displacement of 2000 mm. Based on the work by Liu and Amdahl [2], it can be estimated that roughly 40% of the maximum possible impact energy will be dissipated in this scenario, which yields 16.25 MJ. If we assume a ship with a size of 150,000 t, the corresponding iceberg size will be 1605 t. In such a case, the ship will mostly crush the iceberg, and no penetration will be initiated. The maximum deflections of the outer and inner shell are 328 mm and 7.5 mm, respectively, which are obtained based on Figures 6 and 8. Other scenarios may follow the same procedure to obtain the extents of damage.

Finally, the following conclusions can be highlighted based on the present numerical study:

- The steel model by Alsos et al.(2009) [5] and the iceberg model by Liu et al. [7] are successfully coupled to simulate the side-ship and iceberg collision;
- The iceberg profiles in the present study have been simplified by revolving a parabolic or a circular line about an axis. An iceberg with a parabolic profile ($y = 1/500\,x^2$) will be crushed by a ship, and an iceberg with a circular line profile ($Y^2 + (X - r)^2 = r^2, r = 3000$ mm) is sufficiently stiff to crush the side structure. When $r = 1000,\ 2000$ mm, the iceberg and side structure share the energy during the collision in the integrated analyses;

- In the rigid analyses, the "sharp" profiles, the first and second profiles ($y = 1/500x^2$ and $Y^2 + (X - 1000)^2 = 1000^2$), penetrate the side structure. In the integrated analyses, no fracture is observed in the side structure in all cases;
- The collision location shows significant influence when both the iceberg and side structure endure large deformation, for example, the second and third groups (I-C-1000-A,B,C and I-C-2000-A,B,C). The web frame and stringer provide support for types A and C and increases the side structure stiffness significantly compared to type B, where the location of collision is in the middle of the spacing;
- The integrated analyses differ very much from the rigid analyses in most cases. Moreover, the difference is highly dependent on the iceberg profiles. The iceberg with a "sharp" profile shows the greatest difference, while the "blunt" profile shows little difference. In the present study, when the radius of the circle profile is greater than 2000 mm, the iceberg will be as stiff as it is rigid; thus, the rigid analysis is valid in such cases.
- However, it is still quite difficulty to quantify the definitions of "sharp" and "blunt" icebergs. It is recommended to consider the damage of both ship and iceberg at the same time. More work is needed before a general conclusion is derived.

Acknowledgement

This work was carried out through the collaboration of the programmes "ScenaRisC&G" and "PetroArctic" at NTNU, both funded by the Norwegian Research Council. The authors wish to thank the Norwegian Research Council for supporting this research.

References:

[1] Terndrup Pedersen P. and S. Zhang, *On Impact mechanics in ship collisions.* Marine Structures, 1998. 11(10): p. 429-449.

[2] Liu Z. and J. Amdahl, *A new formulation of the impact mechanics of ship collisions and its application to a ship-iceberg collision.* Marine Structures, 2010. 23(2010): p. 360-384.

[3] Liu Z., J. Amdahl, and S. Løset. *Numeric simulation of collisions between ships and icebergs*. *International Conference on Port and Ocean Engineering Under Arctic Conditions*. 2009. Lulea, Sweden.

[4] Liu Z., J. Amdahl, and S. Løset. *Integrated numerical analysis of an iceberg collision with a foreship structure.* Marine Structures (in press).

[5] Alsos H.S., J. Amdahl, and O.S. Hopperstad, *On the resistance to penetration of stiffened plates, Part II: Numerical analysis.* International Journal of Impact Engineering, 2009. 36(7): p. 875 - 887.

[6] Alsos H.S. and J. Amdahl, *On the resistance of tanker bottom structures during stranding.* Marine Structures, 2007. 20(4): p. 218 - 237.

[7] Liu Z., J. Amdahl, and S. Loset, *Plasticity based material modelling of ice and its application to ship-iceberg.* Cold Regions Science and Technology, 2011. 65(3): p. 326-334.